Investigating Elevation, Terrain, and Regional Corrections to Gravity Survey Data

Fazlie Latib, *Department of Geoscience, University of Calgary*

Abstract

To understand the basic of analysing gravity data, a code was developed in MATLAB to perform elevation, terrain, and regional corrections to gravity survey data (that has been applied to theoretical, tidal and instrument drift corrections from previous study). The elevation-dependent corrections involved in this study are the free-air and Bouguer plate corrections. The elevation-dependent corrections are applied one by one in order. At each point, the contour plot of the gravity is plotted. The irregular contour lines after applying drift correction changed into smoothed contour lines after applying the free-air correction. Both the contour plots after applying the free-air and Bouguer corrections looks the same to each other. The presence of an ore deposit (gravity anomaly) can be seen on the contour plot after the terrain correction is applied. The same can be seen after the regional correction is applied. The contour plots of $\partial g/\partial x$, $\partial g/\partial y$ and $\partial^2 g/\partial z^2$ are created to observe the lateral extent of the anomaly in n the east-west and north-south directions. After locating the coordinate of the highest concentrations of mass (Easting 2 km, Northing 49 km) from the highest gravity anomaly point, the total mass of the anomalies below this point at a depth of approximately 500 m relative to the datum (2948 m) is calculated to be 2.57×10^{15} kg.

Background / Theory

Gravity method is a versatile geophysical technique used to detect and identify subsurface bodies and anomalies within the Earth. This method has been used extensively in the hydrocarbon and mineral exploration over the years. Gravity surveys exploit the very small changes in gravity from place to place that are caused by changes in subsurface rock density (Telford et al., 1990). Higher gravity values are found over rocks that are denser, and lower gravity values are found over rocks that are less dense. A buried body represents a subsurface zone of anomalous mass and causes a localized perturbation in the gravitational field known as a gravity anomaly.

The acquisition of gravity data is done using a gravity meter or gravimeters where it measures the variations in the Earth's gravitational field. Most commonly used gravimeters measured the spatial and temporal change in gravity or its gradient rather than the absolute value of gravity intensity. This is due to the high sensitivity requirement of absolute measurements, which is of the order of 10^{-8} for 0.01 mGal resolution, compared with a significantly lower sensitivity requirement for relative instruments. Virtually all modern exploration gravimeters used in this way are based on the zero-length spring principle originally developed by LaCoste (1934) where the zero-length spring is used since they have tension proportional to absolute length, rather than to extension from unstressed length.

To make accurate measurements, the instrument must be level (aligned with the vector of the Earth's gravity field), in a place quiet enough to avoid vibrations (e.g., trucks rumbling by and earthquakes). The instrument should also be brought to the specified temperature a few days or at least several hours prior to the start of the survey to remove temperature gradients within the meter and achieving thermal and mechanical equilibrium to avoid sharp changes in temperature that effect the instrument's metal parts.

Gravity corrections is applied to observed or measured gravity data because the gravity varied for many reasons other than lateral variations in mass in the subsurface where gravity can also vary with latitude due to the shape and rotation of the Earth, the tides, and with variations in elevation. Other than theoretical and time-dependent (tidal and instruments drift) corrections that were previously applied, elevation-dependent (free-air and Bouguer plate) and terrain corrections also have to be applied to the gravity data.

The free-air correction accounts for gravity variations caused by the difference in elevation between the base station and the measurement point and can be calculated using Equation 1. However, the free air correction only accounted for changes in gravity because of distance from the centre of mass of the Earth but did not account for the presence of material in between. Hence, the Bouguer correction is then needed.

$$\Delta g_{FA} = -\frac{GM_e \Delta Z_i}{R_e^3} \approx -0.3086\ \Delta Z_i \text{ mGal/m} \quad (1)$$

The Bouguer plate correction accounts for the mass of average crust between the base station, or reference ellipsoid, and the measurement point, given the height difference between them. If the measurement point located on the Earth's surface is above the reference ellipsoid, then the "extra" mass of rock between the station and reference ellipsoid has the effect of increasing gravity. Similarly, if a measurement station is located at an elevation below the reference ellipsoid, then rock is "missing" that would theoretically be pulling up on the meter, with the effect of reducing gravity at that measurement station. The goal of the simple Bouguer correction is to remove this effect of "excess" and "missing" mass, using a formula based on a simple shape – the infinite slab. Assuming that there is a slab of material extending infinitely in all directions with a uniform density ρ_B, we can compute the Bouguer plate correction as shown in Equation 2.

$$\Delta g_{BP} = 2\pi G \rho_B \Delta Z \approx 0.04193\ \rho_B \Delta Z \text{ mGal/m} \quad (2)$$

The final correction is the terrain correction, which accounts for both the upward pull of surrounding regions of higher elevation and the overestimation of the Bouguer plate correction in regions of lower elevation.

Methods / Algorithm

A set of gravity survey data file, **'goph_547_lab_2_data.mat'**, contains four arrays (**grav_survey_data**, **Xt**, **Yt** and **Zt**). The columns of **grav_survey_data** contain the following information (**base_point**, **day**, **time**, **total_time**, **x**, **y**, **z**, **g** and **dg_tide**) where the description of each information is given in Table 1. The other arrays **Xt**, **Yt** and **Zt** contain terrain survey data over a much wider region (±50 km to each side of the gravity survey region). The **Xt** and **Yt** matrices contain the eastings and northings, respectively, of each survey point in km and **Zt** contains the elevation data in metres ASL. Terrain survey points in **Xt**, **Yt** and **Zt** overlapping with the gravity survey region contain identical data. This data comes from a survey that was performed over a 50 km × 50 km region centred on a latitude of 49.1286°N where the presence of an ore deposit with significant density contrast to the surrounding rock at a depth of approximately 750 m was revealed by a prospecting borehole.

Table 1 Description of the information contained in the columns of **grav_survey_data**.

Column	Information	Description
1	**base_point**	An integer indicating whether that survey point was at the base station. If **base_point==1**, the point was at the base station at the beginning of a loop. If **base_point==2**, the point was at the base station at the end of a loop. Otherwise, the point was not at the base station.
2	**day**	A number indicating the day of the survey operation.
3	**time**	The time (in hours) on a given day.
4	**total_time**	The running time (in hours) of the survey starting at midnight on day 1. Note that operations began at just after 8:30AM on day 1, so the first survey point is not at **total_time == 0**.
5	**x**	The easting of the survey location in km.
6	**y**	The northing of the survey location in km.
7	**z**	The elevation (relative to sea level) of the survey point in km.
8	**g**	The measured gravity effect (in μGal) at the survey point. The first data point **g(1)** is the value of absolute gravity at the base station for the first survey measurement, calibrated to a measure of absolute gravity obtained using an absolute gravimeter used to occupy the base station. All subsequent values in column 8 are Δg values relative to the first data point. That is for each data point $i > 1$, $g_i = g_1 + \Delta g_i$ where g_1 is the value in the first row of column 8 and Δg_i is the value in row i of column 8.
9	**dg_tide**	The tidal variation (in μGal) obtained from regular measurements with an absolute gravimeter occupying the base station. The values are calibrated so that when the measured value of absolute gravity matches that from the IGF (i.e. $g_{abs} = g_t$), $\Delta g_{tide} = 0$. That is, these are tidal variations relative to g_t.

The final **g_corr** after applying the theoretical and time-dependent (tidal and instrument drift) corrections from previous investigation is saved to be corrected further here. **Xg**, **Yg** and **Zg** from previous investigation are saved and used here.

The free-air correction (**dg_FA**) is computed using Equation 1 where ΔZ = **Zg – z_datum** (**Zg** is a grid of elevations of each survey point and **z_datum = 2948 m** is the mean elevation value obtained from previous investigation). **Dg_FA** is converted into a grid with the number of rows and columns in the output equal to **Nx** and **Ny** respectively using **reshape()**. **g_corr** is updated by subtracting **dg_FA** from **g_corr** and the current value of **g_corr** is saved as **g_FA**. A contour plot of **g_FA** on the grid defined by **Xg** and **Yg** is created using **contourf()**.

The Bouguer plate correction (**dg_BP**) is computed using Equation 2 where the surface material is assumed to has an average density of $\rho_B \approx 2650$ kg/m^3 and ΔZ = **Zg – z_datum**. **Dg_BP** is converted into a grid with the number of rows and columns in the output equal to **Nx** and **Ny** respectively using **reshape()**. **g_corr** is updated by subtracting **dg_BP** from **g_corr** and the current value of **g_corr** is saved as **g_elev**. A contour plot of **g_elev** on the grid defined by **Xg** and **Yg** is created using **contourf()**.

The terrain correction (**dg_terrain**) array is initialized to zeros with the same dimensions as **g_corr** (and **Xg**, **Yg** and **Zg**). Using a for loop, for each point in **dg_terr**, its x and y coordinates is taken from **Xg** and **Yg** while the z coordinate is set as **z_datum**. The coordinates is saved as **xi**. Using a for loop within the loop before, for all points in the terrain survey data (**Xt**, **Yt**, **Zt**), the coordinates of the local centre of mass (relative to the datum) is saved as the corresponding values from **Xt**, **Yt** and **0.5*(Zt – z_datum)** in a row vector **xm**. The mass of the terrain above or below the datum is computed as **dm = rho_B * (Zt – z_datum) * dA** where **dA = dX*dY** is the area of the current terrain cell and **dX** and **dY** are the grid spacing in the east-west and north-south directions. the gravity effect of that part of the terrain on the current survey point is calculated using the function **grav_eff_point** from Lab Assignment #1 with the inputs **xi**, **xm**, **dm** and **G** where **G** is the gravitational constant ($G \approx 6.674 \times 10^{-11}$ N m^2 kg^{-2}). Then, the current value of **dg_terr** is incremented by the absolute value of the gravity effect computed before.

dg_terr unit is converted from m/s^2 to μGal. **g_corr** is updated by adding **dg_terr** to **g_corr** and the current value of **g_corr** is saved as **g_terr**. A contour plot of **g_terr** on the grid defined by **Xg** and **Yg** is created using **contourf()**.

To eliminate the regional variations of the geoid relative to theoretical gravity (on wavelengths much larger than the 50 km × 50 km of this survey), the regional correction (**dg_rgnl**) is computed as the average of all gravity effect values in **g_corr**. **g_corr** is updated by subtracting **dg_rgnl** from **g_corr** and the current value of **g_corr** is saved as **g_anom**. A contour plot of **g_anom** on the grid defined by **Xg** and **Yg** is created using **contourf()**.

Finally, the contour plots of $\partial g/\partial x$, $\partial g/\partial y$ and $\partial^2 g/\partial z^2$ are created. Assuming that the anomalies are centred at a depth of approximately 500 m relative to your datum, the total mass of the anomalies below the points of highest concentration of gravity effect is estimated.

Results and Discussion

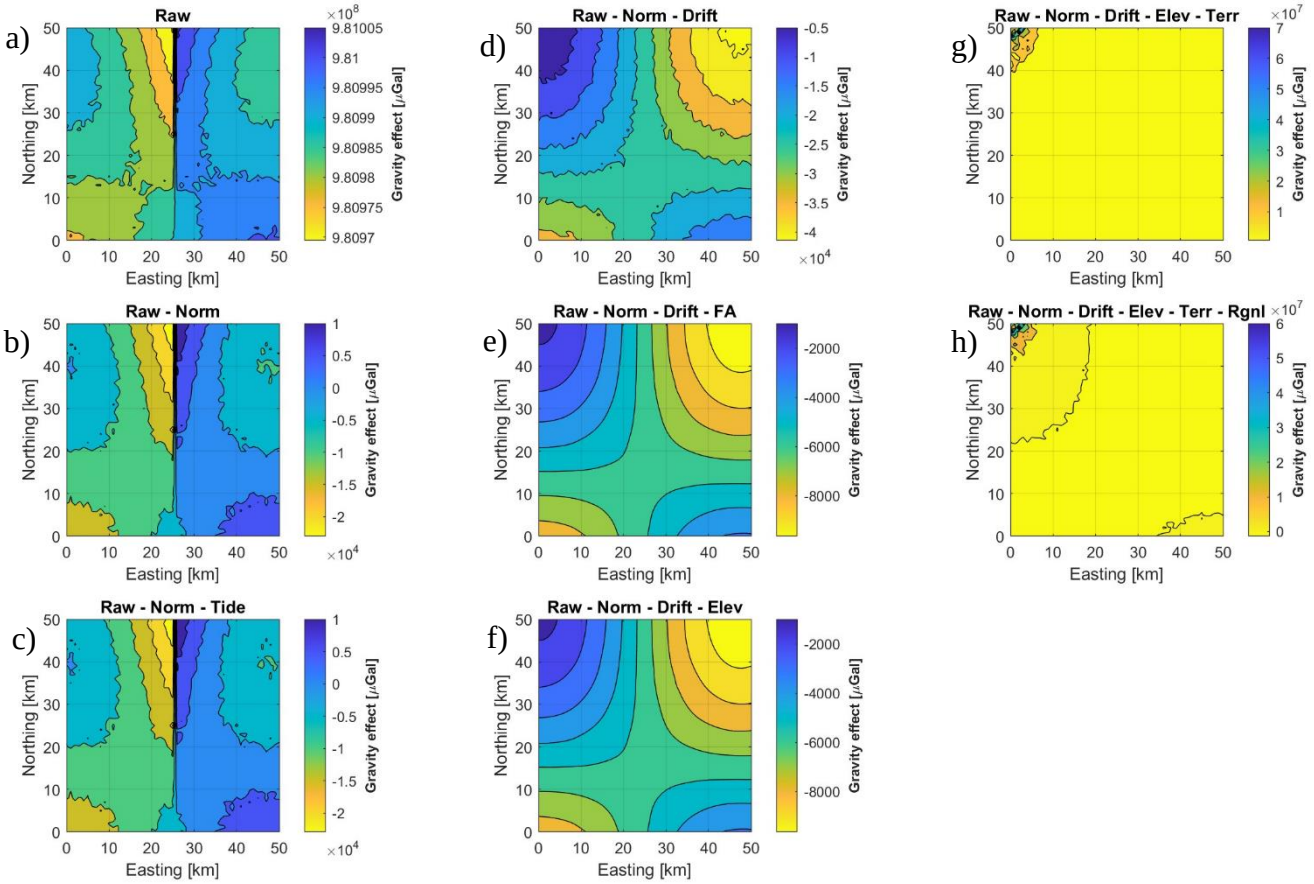

Figure 1 Contour plots of a) the raw gravity data, and the corresponding contour plots in order after applying b) the theoretical gravity, c) tidal correction, d) instrument drift correction, e) free-air correction, f) Bouguer correction, g) terrain correction, and h) regional correction.

When **Zg > z_datum**, the free-air correction will increase **g_corr**. This is because the correction is added to the gravity data for stations above (or at higher elevation than) the datum. As gravity decreases with height above the surface, points above datum are corrected back to the value they would have at datum by adding in this correction. When **Zg > z_datum** for the Bouguer correction, it will decrease **g_corr**. This is because the correction is subtracted to the gravity data for stations above (or at higher elevation than) the datum. The excess mass underlying observation points located at elevations higher than the elevation datum would cause an increase in the gravity measurement, hence the gravity increase due the effect of the mass has to be subtracted.

Figure 1 shows the contour plot of the raw data before (Figure 1a) and after certain corrections. After applying the free-air correction, the contour plot (Figure 1e) does not look very different to the contour plot after applying the drifts correction (Figure 1d) where the irregular contour lines in Figure 1d becomes smooth contour lines in Figure 1e. After the Bouguer plate correction is applied, the contour plot (Figure 1f) looks very similar to the contour plot after applying the free-air correction (Figure 1e).

Figure 1g shows the contour plot after terrain correction is applied. This plot is very much different that all the previous plots, where from this plot, the presence of an ore deposit (anomaly) can be seen clearly located at the top left corner of the plot. This can be deduced because there is only a small area of the plot that has high gravity effect (around 2.5 to 7 μGal – green to dark blue shaded area). The contour plot after applying the regional correction (Figure 1g) shows the same anomaly area as Figure 1g.

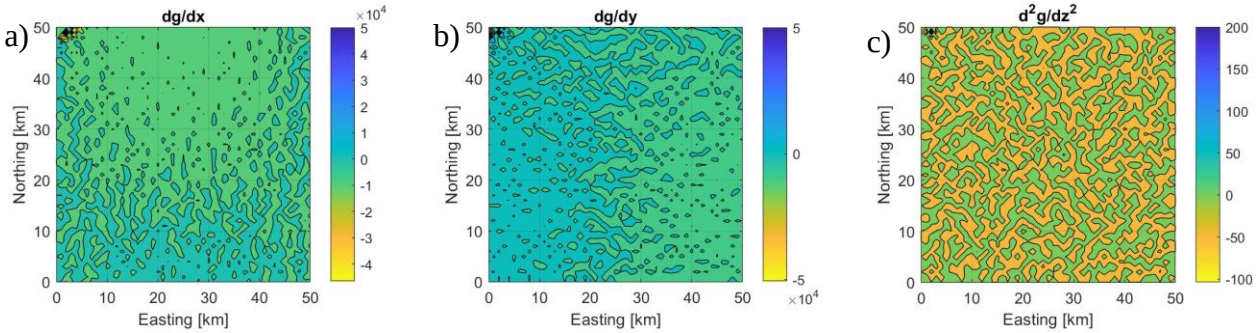

Figure 2 Contour plots of $\partial g/\partial x$, $\partial g/\partial y$ and $\partial^2 g/\partial z^2$.

From Figure 2a, the lateral extent in the east-west is found to be ~5km (between Easting 1 to 6 km). From Figure 2b, the lateral extent in the north-south is found to be ~2km (between Northing 48 to 50 km).

The highest concentrations of mass (found from the maximum gravity effect) seem to be located below the coordinate of Easting 2 km and Northing 49 km. Assuming that the anomalies are centred at a depth of approximately 500 m relative to the datum, the total mass of the anomalies below the point of highest concentration of gravity effect is calculated to be 2.57×10^{15} kg.

Conclusion

Gravity surveys are incomplete without further consideration of other variables affecting gravity measurements. The raw gravity data cannot tell the complete information about the subsurface. The results of the investigation define the importance of correction to the data. Previously, the theoretical and time-dependent correction is applied. In this study, the free-air, Bouguer plate and elevation correction is applied. As a result, the gravity anomaly can be observed which can be directly related to the presence of ore deposit in the area.

References

Telford, W.M., Geldart, L.P., Sheriff, R.E. and Keys, D.A. (1990) Applied Geophysics (2nd edn), Cambridge